

Incommensurate dynamic correlations in the quasi-two-dimensional spin liquid BiCu_2PO_6

K.W. Plumb,^{1,*} Zahra Yamani,² M. Matsuda,³ G. J. Shu,⁴ B. Koteswararao,⁴ F.C. Chou,⁴ and Young-June Kim^{1,†}

¹*Department of Physics, University of Toronto, Toronto, Ontario M5S 1A7, Canada*

²*Canadian Neutron Beam Centre, National Research Council,*

Chalk River Laboratories, Chalk River, Ontario, K0J 1P0, Canada

³*Quantum Condensed Matter Division, Oak Ridge National Laboratory, Oak Ridge Tennessee 37831, USA*

⁴*Center for Condensed Matter Sciences, National Taiwan University, Taipei, 10617 Taiwan*

(Dated: October 31, 2018)

We report detailed inelastic neutron scattering measurements on single crystals of the frustrated two-leg ladder BiCu_2PO_6 , whose ground state is described as a spin liquid phase with no long-range order down to 6 K. Two branches of steeply dispersing long-lived spin excitations are observed with excitation gaps of $\Delta_1 = 1.90(9)$ meV and $\Delta_2 = 3.95(8)$ meV. Significant frustrating next-nearest neighbor interactions along the ladder leg drive the minimum of each excitation branch to incommensurate wavevectors $\zeta_1 = 0.574\pi$ and $\zeta_2 = 0.553\pi$ for the lower and upper energy branches respectively. The temperature dependence of the excitation spectrum near the gap energy is consistent with thermal activation into singly and doubly degenerate excited states. The observed magnetic excitation spectrum as well as earlier thermodynamic data could be consistently explained by the presence of strong anisotropic interactions in the ground state Hamiltonian.

PACS numbers: 75.10.Jm, 75.10.Kt, 75.40.Gb

I. INTRODUCTION

Low-dimensional quantum antiferromagnets can realize a rich and diverse array of physical phenomena from a seemingly simple set of interactions. The canonical low-dimensional quantum antiferromagnet is the spin-1/2 Heisenberg chain, in which neighboring spins are coupled with antiferromagnetic exchange J_1 . The system does not have any long range order and the spin-spin correlations decay with a power law. In spin-1/2 chains the elementary excitations are $S = 1/2$ quasiparticles termed spinons and the dynamic susceptibility is dominated by a gapless dispersive continuum.^{1,2} Frustration can be introduced to the spin-1/2 chain by competing antiferromagnetic next-nearest-neighbor (NNN) interaction J_2 . For a large NNN exchange of $J_2/J_1 > 0.241$ the ground state is composed of dimerized singlets^{3,4} and the excitation spectrum is described with a coherent triplet band of gapped excitations. At the Majumdar-Ghosh (MG) point $J_2/J_1 = 0.5$ the singlet ground state is exact and the system forms a one-dimensional dimer crystal.⁵ As the NNN exchange is increased beyond the MG point frustration drives the spin correlations in the dimerized system to an incommensurate wavevector.^{6,7}

A gap may also be introduced into the excitation spectrum by coupling two neighboring chains via a short range interaction J_{rung} , to create an even leg ladder⁸. The rung coupling confines spinons into $S=1$ magnons and the low energy dynamic susceptibility exhibits a well defined, triply degenerate, single particle peak.⁹ Theoretical understanding of the properties of even-leg ladders is highly developed⁹⁻¹¹ and a number of experimental realizations have allowed for a detailed understanding of the very rich physical phenomena present in spin-ladders for both the strong rung coupling (rung-singlet)¹²⁻¹⁴ and

strong-leg coupling (Haldane)^{15,16} regimes. However, the physics of spin ladders with additional frustrating NNN interactions is not understood well. Field theoretical and numerical investigations have indicated that the addition of frustration can lead to many exotic quantum ground states not realized in the standard two-leg ladder,¹⁷⁻¹⁹ yet comprehensive experimental investigations are still lacking.

Such a frustrated two-leg ladder seems to be realized in a newly discovered quasi-two-dimensional spin-1/2 compound BiCu_2PO_6 .^{20,21} The crystal structure of BiCu_2PO_6 is shown in Fig. 1. Zig-zag chains of Cu^{2+} ions run parallel to the crystallographic b-axis, as shown clearly by a projection in the $\mathbf{a}-\mathbf{b}$ plane in Fig. 1 (c). Along the chains Cu^{2+} ions at crystallographically inequivalent sites, labeled Cu_A and Cu_B , interact via NN antiferromagnetic exchange J_1 and NNN antiferromagnetic exchange J_2 . The chains are coupled along the c-axis by both J_3 and J_4 . Although the J_3 interaction distance is shorter than J_4 , band structure calculations predict J_4 to be the dominant coupling along the c-axis.²³ Structurally, this is a result of the particular superexchange pathways. J_3 is a nearly 90° Cu-O-Cu bond, which is usually small and ferromagnetic, in contrast J_4 is mediated by a nearly 180° Cu-O-O-Cu bond. Therefore, BiCu_2PO_6 can be considered as a system of J_1 - J_2 - J_4 ladders with a weaker interladder coupling J_3 .^{21,23}

Magnetic susceptibility, magnetization, and heat capacity measurements on powder samples have consistently reported that BiCu_2PO_6 has a singlet ground state with a spin excitation gap of ~ 2.9 meV.^{20,22-24} The thermodynamic measurements cannot be interpreted in terms of simple gapped one-dimensional (1D) models, including the J_1 - J_2 chain and the two-leg ladder, but require a combination of frustration and two-leg-

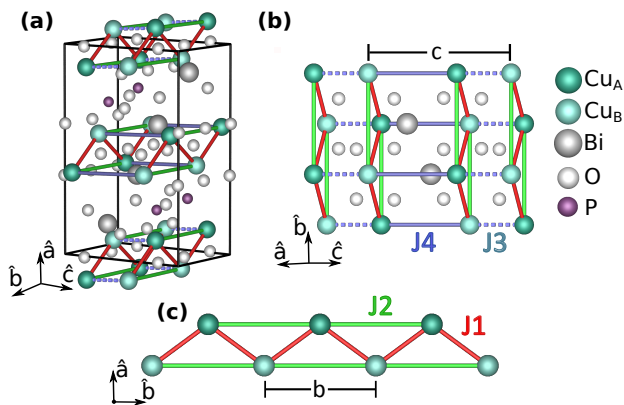


FIG. 1. (a) Schematic representation of the crystal structure of BiCu_2PO_6 . The unit cell is orthorhombic, space group Pnma with $a = 11.755 \text{ \AA}$, $b = 5.16 \text{ \AA}$, $c = 7.79 \text{ \AA}$ at 6 K .²² (b) Perspective view of the ladder unit in the b - c plane and (c) projection into the a - c plane showing the zigzag chains of Cu^{2+} ions.

ladder geometry.^{21,24} Inelastic neutron scattering (INS) measurements on powder samples have reported that BiCu_2PO_6 has a dispersive spin excitation spectrum with a gap of $\Delta = 2.9 \text{ meV}$ and that significant frustration is required to describe the powder averaged structure factor.²¹ More recent high field magnetization measurements on single crystals have revealed that the critical field for the closing of the spin gap is dependent on the direction of the applied field indicative of strong anisotropic interactions in the magnetic Hamiltonian.²⁵

In real materials (usually) small anisotropic interactions, additional to the Heisenberg exchange couplings, invariably exist. Such interactions are often a negligible perturbation to the isotropic Heisenberg interaction, as in cuprate superconductors^{26,27}, but can sometimes alter the magnetic properties in a fundamental way. As an example, for compounds that lack local inversion symmetries anisotropic Dzyaloshinsky-Moriya (DM)^{28,29} interactions are permitted in the magnetic Hamiltonian. Depending on the particular crystallographic symmetries the DM interaction can induce a staggered field.³⁰ In 1D chains this staggered field results in an effective confinement potential between spinons and the appearance of incommensurate gapped modes on application of a magnetic field.³⁰ The staggered field also has a drastic effect for spin ladders. In contrast to a spin ladder in a uniform magnetic field, which transitions to a gapless phase above a critical field, the presence of a staggered field is predicted to lead to a quantum phase transition between two gapped phases above and below the critical field.³¹

The numerous exchange pathways in BiCu_2PO_6 complicate interpretation of thermodynamic data and important details including interladder coupling and anisotropic interactions are often neglected in the analysis. In order to determine the microscopic spin Hamiltonian of a complex magnetic system with competing interactions and anisotropic exchange cou-

plings, INS measurements using a single crystal sample are essential.

We have conducted an extensive neutron scattering study of the magnetic excitation spectrum in BiCu_2PO_6 . Our data confirms that BiCu_2PO_6 is appropriately described by weakly interacting two-leg ladders with incommensurate dynamic correlations driven by frustration. In contrast to the single triply degenerate excitation branch expected for an isotropic ladder, we observe two branches of steeply dispersing, long-lived, excitations. The excitation gap of each mode, directly probed by INS, was measured to be $\Delta_1 = 1.90(9) \text{ meV}$ and $\Delta_2 = 3.95(8) \text{ meV}$, this differs significantly from the $\sim 2.9 \text{ meV}$ gap extracted from thermodynamic measurements^{20,22,23} indicating that current models are inadequate to describe the ground state of BiCu_2PO_6 . Furthermore, the temperature dependence of the incommensurate modes are consistent with a description in terms of thermal activation into singly and doubly degenerate modes. We argue that, in addition to frustration, strong anisotropic interactions are important for understanding the physics of this material.

II. EXPERIMENTAL DETAILS

Experiments were carried out on a 4.5 g single crystal sample grown using the traveling floating zone method. The sample mosaic was measured by neutron scattering to be 0.2° at $T = 6 \text{ K}$. Measurements were performed on the C5 DUALSPEC triple axis spectrometer at the Canadian Neutron Beam Centre at Chalk River Laboratories and on the HB1 triple axis spectrometer at HFIR. Both instruments employed a vertically focusing pyrolytic graphite (PG) monochromator and C5 was equipped with a flat graphite analyzer while HB1 utilized a fixed vertically focusing analyzer. On C5 the sample was mounted in the $(0, k, l)$ scattering plane and the spectrometer was operated at a fixed final energy of 14.56 meV . Experiments on HB1 were performed with the sample mounted in the $(h, k, 2k)$ horizontal scattering plane at a fixed final energy of 14.7 meV . Temperature control was provided by a closed cycle cryostat. All data was corrected for higher-order wavelength neutrons in the incident beam monitor.³² Intensities were placed on an absolute scale by normalization with the integrated intensity of a transverse acoustic phonon measured near the (004) Bragg peak on the respective instrument.

The crystallographic unit cell of BiCu_2PO_6 is orthorhombic, space group Pnma with $a = 11.755 \text{ \AA}$, $b = 5.16 \text{ \AA}$, $c = 7.79 \text{ \AA}$. Along the zig-zag chains NN Cu^{2+} ions in BiCu_2PO_6 are separated by $b/2$ so that the momentum of magnetic excitations in the \mathbf{b}^* direction is indexed using $\bar{\mathbf{k}} = \mathbf{q} \cdot \mathbf{b}/2 = \pi\mathbf{k}$.

III. EXPERIMENTAL RESULTS

A. Spin excitation spectra

The momentum and energy dependence of spin excitations in BiCu_2PO_6 were surveyed through a series of constant- \mathbf{Q} scans. No evidence for elastic magnetic scattering at $T = 6$ K was found indicating the absence of static magnetic order in BiCu_2PO_6 . Representative scans taken in proximity of the spin gap at $T=6$ K are shown in Fig. 2. Throughout most of the Brillouin zone the

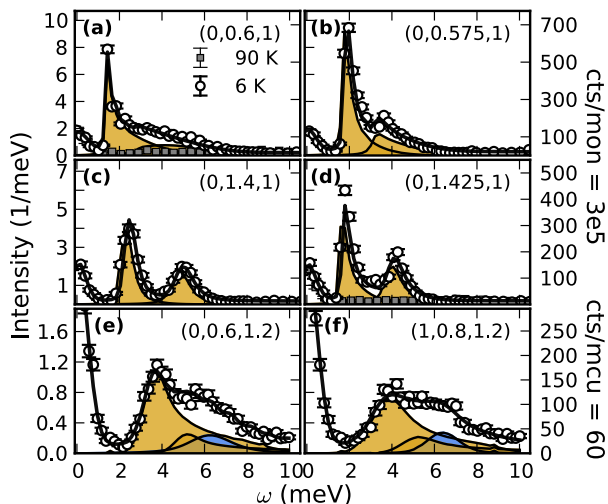


FIG. 2. Representative constant- \mathbf{Q} scans. Data in panels (a)-(d) were obtained on C5 with the sample aligned in the $(0, k, l)$ scattering plane and a collimation of $33^\circ\text{-}48^\circ\text{-}51^\circ\text{-}144^\circ$. Data in panels (e) and (f) was obtained on HB1 with the sample aligned in the $(h, k, 2k)$ scattering plane and a collimation of $48^\circ\text{-}40^\circ\text{-}40^\circ\text{-}120^\circ$. All data was collected at $T = 6$ K. The solid black lines are the results of a global fit to the single mode approximation, gold and blue filled areas show the contribution from each mode including resolution effects.

scattering intensity is dominated by two well defined and highly dispersive modes. The dispersion of these modes is not commensurate with the structural unit cell and the scattering intensity vanishes as the temperature is increased above 60 K, where a broad maxima in the magnetic susceptibility was observed²⁰, confirming the magnetic origin. Extensive sampling of \mathbf{Q} -values throughout reciprocal space enabled the construction of a map of the dynamic structure factor $S(\mathbf{q}, \omega)$ shown in Fig. 3 (a) - (c).

Magnetic excitations in BiCu_2PO_6 are highly anisotropic, with a bandwidth of ~ 12 meV in the \mathbf{b}^* direction and ~ 2 meV in the \mathbf{c}^* direction. Dispersion along the \mathbf{c}^* direction confirms the presence of a sizable interladder interactions. Any dispersion along the \mathbf{a}^* direction could not be resolved by our thermal triple axis measurements, indicating that BiCu_2PO_6 should be regarded as a quasi-two-dimensional system.

Within the first Brillouin zone, each branch of the ex-

citation spectrum has two minima occurring at wavevectors $\zeta_\alpha = 0.5 + \delta_\alpha$ and $\zeta_\alpha = 1.5 - \delta_\alpha$. The distinct double-well structure is reminiscent of the dispersion in J_1 - J_2 chains and the incommensurate minima is indicative of a strong competition between J_1 and J_2 .^{6,7,17,19}

The excitation spectrum shown in Fig. 3(a) cannot be described using strong-coupling expansions for a two-leg ladder with competing interactions.^{19,23} These perturbative expansions require that the rung coupling (J_4) is much larger than the coupling along the chains (J_1, J_2). The large bandwidth of each branch compared with the gap energies implies that BiCu_2PO_6 likely lies in an intermediate coupling regime where $J_1 \sim J_4$, this is in qualitative agreement with band-structure calculations.²³

Lacking a microscopically motivated theory for BiCu_2PO_6 , the essential features of the lowest energy excitations were determined by fitting data in the vicinity of the dispersion minimum with a single mode approximation (SMA) cross-section and an empirical dispersion relation:

$$(\omega_{\mathbf{q}}^\alpha)^2 = \Delta_\alpha^2 + v_\alpha^2 \sin^2(\tilde{k} - \pi\zeta_\alpha), \quad (1)$$

$$S(\mathbf{q}, \omega) = \frac{1}{1 - e^{-\omega_{\mathbf{q}}^\alpha/T}} \frac{\mathcal{A}_{\mathbf{q}}^\alpha}{\omega_{\mathbf{q}}^\alpha} \delta(\omega - \omega_{\mathbf{q}}^\alpha), \quad (2)$$

$\mathcal{A}_{\mathbf{q}}^\alpha$ is a mode dependent intensity pre-factor, v_α parameterizes the spin-wave velocity of each mode, and we set $\hbar = k_B = 1$ throughout this paper. Equation (2) was convolved with the instrumental resolution function^{33,34} and globally fit to scans in the range $0.5\pi < \tilde{k} < 0.7\pi$ and $1.3\pi < \tilde{k} < 1.5\pi$, only $\mathcal{A}_{\mathbf{q}}^\alpha$ was allowed to vary between scans. Incoherent background was modeled as a constant plus a Gaussian function centered on $\omega = 0$. The broad peak widths and \mathbf{Q} -dependence of lineshapes visible in Fig. 2 (a)-(d) and Fig. 3 (a)-(b) are accounted for entirely by resolution effects and two steeply dispersing modes indicating that the excitations are long-lived. Additional intensity appears in $(h, k, 2k)$ plane which is best accounted for by a damped harmonic oscillator, blue shaded area in Fig. 2 (e) and (f).³⁵ Dispersion parameters determined from the low-energy global fit were: $\Delta_1 = 1.90(9)$ meV, $\Delta_2 = 3.95(8)$ meV, $v_1 = 16.4(1.4)$ meV, $v_2 = 19.6(1.7)$ meV, $\delta_1 = 0.074(2)$, $\delta_2 = 0.053(4)$. Scans simulated using these parameters are shown as solid lines in Fig. 2 and the resulting dispersion is plotted as solid and broken grey lines in Fig. 3 (a).

The incommensurate wavevector of the lower branch $\zeta_1 = 0.574\pi$ can be used to estimate the ratio J_2/J_1 in the two limits of strong rung coupling $J_4 > J_1$ and uncoupled weakly interacting J_1 - J_2 chains. For strong rung coupling the wavevector minimizing the dispersion can be estimated exactly¹⁹

$$\zeta = \arccos\left(\frac{-J_1}{4J_2}\right), \quad (3)$$

giving $J_2/J_1 = 1.08$. In the opposite limit of isolated J_1 - J_2 chains, density matrix renormalization group

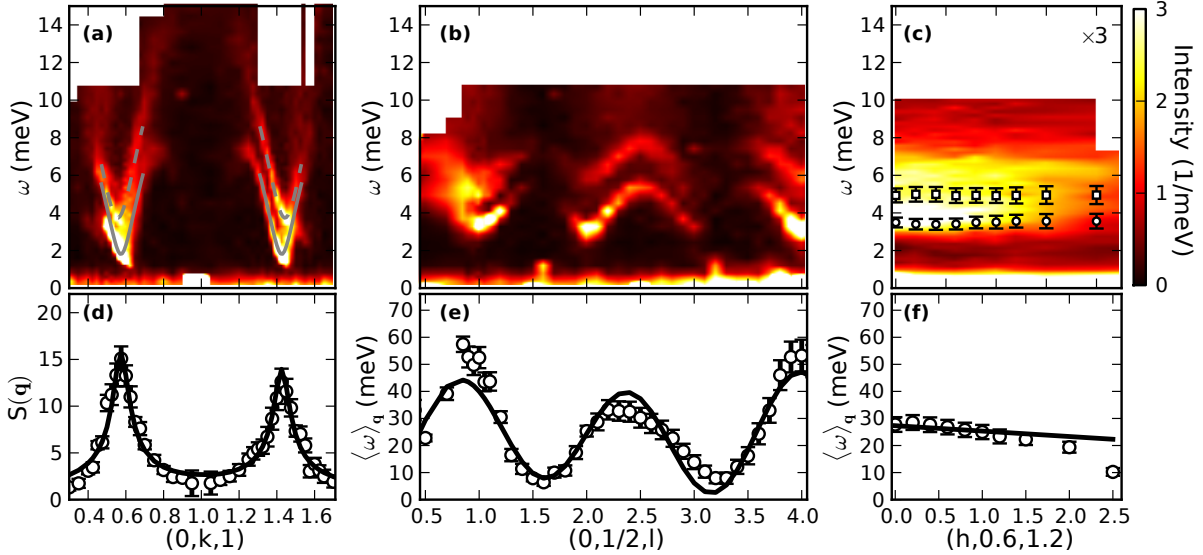


FIG. 3. (a) - (c) Inelastic neutron scattering intensity map for $T = 6\text{K}$ constructed by linear interpolation of a series of constant scans. All data have been corrected for the isotropic Cu^{2+} form factor. Solid and dashed gray lines show the dispersion relation, Eq. (1), using the parameters obtained from the single mode approximation fit. Solid white symbols in (c) show the fitted peak positions of resolution limited mode. (d) Structure factor data obtained at $T = 6\text{K}$, for equal-time spin correlations along the chain \mathbf{b}^* direction, calculated by numerically integrating constant \mathbf{q} scans for $\omega > 0.5\text{ meV}$. (e) - (f) Measured first moment as a function of wavevector along the rung \mathbf{c}^* direction and perpendicular to the planes of the ladders, along \mathbf{a}^* . Solid lines are fits as described in the text.

(DMRG) results⁷ can be used to estimate J_2/J_1 from ζ giving $J_2/J_1 \approx 0.88$. Our INS data situates BiCu_2PO_6 in an intermediate coupling regime; however, the two limits of isolated chains and strong rung coupling tightly constrain $J_2 \approx J_1$.

Information about the length scales associated with spin correlations can be extracted from the equal-time structure factor, shown in Fig. 3 (d). It was calculated by numerically integrating constant \mathbf{q} scans between 0.5 and 15 meV, all scans were corrected for the isotropic Cu^{2+} form-factor prior to integration.³⁶ Static correlations in BiCu_2PO_6 are well described by a double peaked square root Lorentzian, characteristic of spin chains with competing NN and NNN interactions and exponentially decaying spin-spin correlations³⁷

$$S(k) \propto \frac{1}{\sqrt{\kappa^2 + (k - \zeta')^2}} + \frac{1}{\sqrt{\kappa^2 + (k - \zeta'')^2}}, \quad (4)$$

where $\zeta' = 0.5 + \delta$, $\zeta'' = 1.5 - \delta$ and $\xi = 1/\kappa$ is the correlation length. Fitting Eq. (4) to data in Fig. 3 (d) yields a spin-spin correlation length of $\xi/(b/2) = 8.0(6)$ and $\delta = 0.074(5)$.

The $\sim 2\text{ meV}$ bandwidth along the \mathbf{c}^* direction implies that there is a significant coupling between the ladder units. However, it is not possible to distinguish either J_3 or J_4 as the inter/intra ladder coupling from the shape of the dispersion alone. More information is contained in the modulation of INS intensity along the \mathbf{c}^* and \mathbf{a}^* directions. In the absence of a microscopic model for

the spin dynamics in BiCu_2PO_6 the first moment sum rule can be utilized to determine the relative contribution of spin-pair correlations across each bond to the ground state energy.^{38,39} For a Heisenberg Hamiltonian the first moment sum rule is written

$$\begin{aligned} \langle \omega \rangle_{\mathbf{q}} &= \int_{-\infty}^{\infty} \omega S^{\alpha\alpha}(\mathbf{q}, \omega) d\omega \\ &= -\frac{1}{3} \sum_{j,j'} J_{jj'} \langle \mathbf{S}_j \mathbf{S}_{j'} \rangle [1 - \cos(\mathbf{q} \cdot \mathbf{r}_{jj'})], \end{aligned} \quad (5)$$

where $\langle S_j^\beta S_{j'}^\beta \rangle$ is the spin-spin correlation across bond $\mathbf{r}_{jj'}$. Within the single mode approximation the dimer-interference term $[1 - \cos(\mathbf{q} \cdot \mathbf{r}_{jj'})]$ accounts entirely for the \mathbf{q} -dependent intensity modulation of the inelastic scattering intensity along the rung direction for a system of isolated ladders^{12,40}. However, the sum rule in Eq. (5) is strictly only valid for a centro-symmetric lattice obeying inversion symmetry, hence must be applied with caution when analyzing the spectrum from BiCu_2PO_6 where a significant DM anisotropy on each rung is potentially present. The first-moment was measured in BiCu_2PO_6 by numerically integrating constant- \mathbf{q} scans along the \mathbf{a}^* and \mathbf{c}^* directions and globally fit to equation (5). All scans were corrected for the isotropic Cu^{2+} form-factor prior to integration.³⁶ The best fit was obtained with $J_3 \langle \mathbf{S}_0 \mathbf{S}_3 \rangle = -12(5)\text{ meV}$, $J_4 \langle \mathbf{S}_0 \mathbf{S}_4 \rangle = -58(2)\text{ meV}$. Intensity modulation along the \mathbf{c}^* and \mathbf{a}^* directions is well described including only bonds J_3 and J_4 the results of the fit are shown as solid lines in Fig. 3

(e) - (f). The intensity modulation is thus consistent with a two-leg ladder formed by antiferromagnetic rung coupling J_4 and weaker interladder coupling J_3 .

Our neutron scattering results confirm that the J_1 - J_2 - J_4 two-leg ladder with interladder exchange J_3 is an appropriate description of BiCu_2PO_6 . However, the gap energy differs significantly from the value of $\Delta \sim 2.9$ meV reported by previous thermodynamic measurements.^{20,21,23} This discrepancy is potentially resolved by the presence of strong anisotropic interactions neglected in the thermodynamic analysis. Indeed, DM anisotropies are permitted by the crystallographic symmetries of BiCu_2PO_6 . These anisotropies can act to split the degeneracy of the lowest lying excitations in zero field, so that the thermodynamic properties are controlled by two gaps. It is notable, if perhaps coincidental, that the 2.9 meV thermodynamic gap is in agreement with the average of the two gaps measured by INS, $1/2(\Delta_1 + \Delta_2) = 2.93(6)$ meV. We have also checked that the low-temperature magnetic specific heat can be fit using an effective 1D model including the sum of contributions from both the low and high energy modes $C_m = 1/2(g_1 \exp(-\Delta_1/T) + g_2 \exp(-\Delta_2/T))$ with each gap fixed at the value determined from INS. Furthermore, a zero-field splitting of the lowest lying excitation resulting from a staggered DM interaction is consistent with the temperature dependence data presented next.

B. Temperature Dependence

The temperature dependence of spin excitations at $\mathbf{q} = (0, 1.425, 1)$ near the incommensurate wavevector is shown in Fig. 4(a). As the temperature is increased the inelastic features broaden and shift to higher energies. Above 25 K the two excitations can no longer be distinctly identified and above 55 K the inelastic signal cannot be distinguished from background. Each spectrum was fit to the resolution convolved single mode cross section [Eq. (2)] with a normalized Lorentzian function in place of the delta function to account for intrinsic broadening of each mode. Lacking detailed measurements of the dispersion for $T > 6$ K the spin wave velocity was assumed to be independent of temperature for all fits. Constant- \mathbf{q} scans were performed at a wavevector where the orientation of the resolution ellipsoid with respect to the slope of the dispersion minimizes any resolution effects. We have also checked that allowing for a temperature dependent spin wave velocity does not affect the results presented here. Figures 4 (b) - 4(c) show the temperature dependence of the gap energy, half-width half-maximum and integrated intensity of each mode.

In accordance with the thermalization of the ground and excited states, the integrated intensity decreases with increasing temperature. The random phase approximation (RPA) for weakly interacting dimers predicts the scattering intensity to scale with the ground-state excited-state population difference $\Delta n(\Delta_\alpha/T) =$

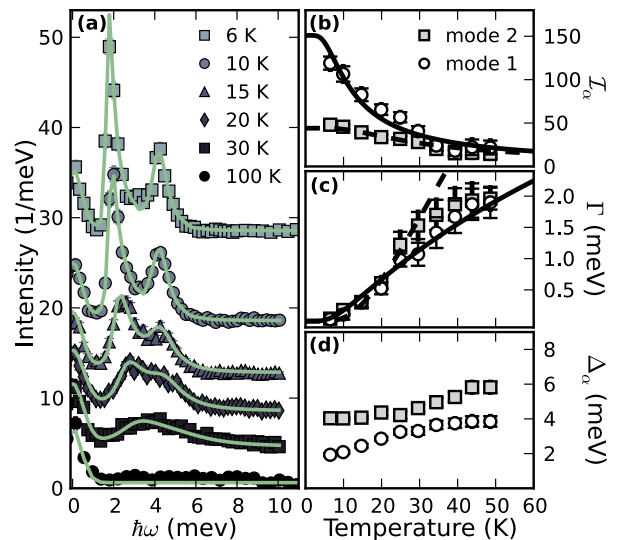


FIG. 4. Temperature dependence of spin excitations near the incommensurate wavevector at $(0, 1.425, 1)$, data collected on C5. (a) A series of representative constant- \mathbf{q} scans, data has been offset for clarity, solid lines are fit to resolution convolved cross-section. (b) - (d) Results of fit to resolution convolved Lorentzian scattering cross-section. Solid and dashed lines in (b) are fit to the population thermalization factor from RPA theory. The solid and dashed lines in (c) are a fit to exponential activated behaviour as described in the text.

$(1 - \exp(-\Delta_\alpha/T)) / (1 + \eta \exp(-\Delta_\alpha/T))$, where η is the degeneracy of the level.⁴¹⁻⁴³ The RPA form is a good description of the data after fitting only an overall scale factor [solid lines in Fig. 4 (b)]. The best fit is obtained assuming the two modes are composed of a lower energy doubly degenerate excitation (Δ_1) and a higher energy singly degenerate excitation (Δ_2). Although we do not have sufficiently detailed data to completely rule out the possibility of two triply degenerate modes. The scaling of the intensities provides good qualitative evidence for the splitting of a single triply degenerate excitation band into a doublet and singly degenerate excitation.

For systems with a gapped excitation spectrum increasing temperature results in an increased density of thermally activated states and concomitantly a decrease in the mean free path between scattering of the excited states, or equivalently a decreased excitation lifetime.⁴⁴⁻⁴⁶ Thus, we expect a thermally induced broadening of the excitation spectrum, as visible in Fig. 4 (c). Below 30 K the damping is consistent with an exponential activated behaviour $\Gamma_\alpha = g_\alpha \sqrt{\Delta_\alpha/T} \exp(\Delta_\alpha/T)$, valid for gapped one-dimensional systems.⁴⁴ The fitted scale factors were $g_1 = 1.05(1)$ and $g_2 = 2.22(16)$ for the low and high energy modes respectively and the fits are shown as solid and dashed lines in Fig. 4(c). A slight increase in excitation energy with increasing temperature was also observed [Fig. 4 (d)]. This is understood in the context of the thermally induced "blue-shift" that has been reported in other quasi-one-dimensional

systems.^{45–49}

IV. DISCUSSION

The excitation spectrum in BiCu_2PO_6 is unique in that competing interactions along the spin chains drive the dynamic correlations to an incommensurate wavevector. Incommensurate dynamic correlations have been observed in the four-leg antiferromagnetic spin tube $\text{Sul} - \text{Cu}_2\text{Cl}_4$ ⁵⁰; however, the degree of incommensurability was much smaller than that observed in BiCu_2PO_6 . Furthermore, the excitations in $\text{Sul} - \text{Cu}_2\text{Cl}_4$ are comprised of a single, triply degenerate mode, while in BiCu_2PO_6 the degeneracy is split and the minimum of each mode occurs at a different wave vector.

In a canonical two-leg ladder the low energy magnetic excitation spectrum is composed of a well defined branch of dispersing triplets. Application of an external magnetic field splits the degeneracy and three branches of excitations may be observed.¹⁵ The degeneracy may also be split in the presence of anisotropic interactions, such as the DM anisotropy, in the microscopic Hamiltonian.^{31,51} We believe that the observed mode splitting in BiCu_2PO_6 may be accounted for by significant staggered DM interactions. In BiCu_2PO_6 local inversion symmetry is broken allowing a DM interaction, with the particular crystallographic symmetries admitting a DM anisotropy with a staggered DM vector on each rung as well as DM interactions on the chain bonds.²³ Although there are many possible DM vectors, our INS measurements can only resolve two-bands of excitations in zero-field indicating that the magnetic Hamiltonian retains a local symmetry, so that we expect a single, dominant, anisotropy term. Indeed DM interactions account for many features of the thermodynamic measurements including the weak linear field dependence of the low field magnetization below H_c ^{23,25}, highly anisotropic critical fields²⁵, and absence of square root singularity in magnetization just above H_c .^{23,51} Field theoretical modeling has shown that staggered anisotropic interactions in a

spin-1/2 two-leg ladder can act to split the lowest lying triplet into a doublet with energy $\Delta_d < \Delta_t$ and higher energy mode with $\Delta_3 > \Delta_t$.³¹ Our temperature dependent measurements are consistent with this scenario, although further detailed magnetic field dependent measurements are required to definitively establish the degeneracy of each mode.

In summary, we have measured the spin excitation spectrum in BiCu_2PO_6 at 6 K. The results confirm that BiCu_2PO_6 is in a quantum disordered phase and that the J_1 - J_2 - J_4 two-leg ladder model with interladder exchange J_3 appropriately accounts for the dominant exchange pathways. The measured incommensurate wavevector $\zeta = 0.574\pi$ allows for an estimate of the relative strength of the competing magnetic interactions $J_2/J_1 \sim 1$. However, the lowest excitation gap is 1.90(9), is significantly lower than the value of 2.9 predicted by thermodynamic measurements. The discrepancy may be explained by the presence of strong anisotropic magnetic interactions which split the excitation spectrum into two coherent branches. We hope that our data will stimulate further theoretical work investigating the effect of Dzyaloshinsky-Moria interactions and frustration on the spin-liquid ground state of a even-leg ladder.

ACKNOWLEDGMENTS

We would like to thank Yong-Baek Kim, Arun Paramakanti, and Leon Balents for useful discussions. Y.J. Kim acknowledges the hospitality and the Aspen Center for Physics supported in part by the National Science Foundation under grant No. PHYS-1066293. Work at the University of Toronto was supported by NSERC of Canada. Work at Chalk River Labs was supported by NSERC of Canada, NRC of Canada. Work at HFIR was sponsored by the Scientific User Facilities Division, Office of Basic Energy Sciences, U.S. Department of Energy. K.W. Plumb acknowledges the support of the Ontario Graduate Scholarship.

* kplumb@physics.utoronto.ca

† yjkim@physics.utoronto.ca

¹ D. A. Tennant, R. A. Cowley, S. E. Nagler, and A. M. Tsvelik, *Phys. Rev. B* **52**, 13368 (1995).

² D. C. Dender, D. Davidović, D. H. Reich, C. Broholm, K. Lefmann, and G. Aeppli, *Phys. Rev. B* **53**, 2583 (1996).

³ F. D. M. Haldane, *Phys. Rev. B* **25**, 4925 (1982).

⁴ K. Okamoto and K. Normura, *Phys. Lett. A* **169**, 433 (1992).

⁵ C. K. Majumdar and D. K. Ghosh, *J. Math. Phys.* **10**, 1388 (1969).

⁶ R. Bursill, G. A. Gehring, D. J. J. Farnell, J. B. Parkinson, T. Xiang, and C. Zeng, *J. Phys. Condens. Matter* **7**, 8605 (1995).

⁷ S. R. White and I. Affleck, *Phys. Rev. B* **54**, 9862 (1996).

⁸ E. Dagotto and T. M. Rice, *Science* **271**, 618 (1996).

⁹ D. G. Shelton, A. A. Nersisyan, and A. M. Tsvelik, *Phys. Rev. B* **53**, 8521 (1996).

¹⁰ S. Gopalan, T. M. Rice, and M. Sigrist, *Phys. Rev. B* **49**, 8901 (1994).

¹¹ T. Giamarchi and A. M. Tsvelik, *Phys. Rev. B* **59**, 11398 (1999).

¹² T. Masuda, A. Zheludev, H. Manaka, L. P. Regnault, J. H. Chung, and Y. Qiu, *Phys. Rev. Lett.* **96**, 047210 (2006).

¹³ V. O. Garlea, A. Zheludev, T. Masuda, H. Manaka, L. P. Regnault, E. Ressouche, B. Grenier, J. H. Chung, Y. Qiu, K. Habicht, K. Kiefer, and M. Boehm, *Phys. Rev. Lett.* **98**, 167202 (2007).

- ¹⁴ B. Thielemann *et al.*, Phys. Rev. Lett **102**, 107204 (2009).
- ¹⁵ T. Hong, Y. H. Kim, C. Hotta, Y. Takano, G. Tremelling, M. M. Turnbull, C. P. Landee, H. J. Kang, N. B. Christensen, K. Lefmann, K. P. Schmidt, G. S. Uhrig, and C. Broholm, Phys. Rev. Lett **105**, 137207 (2010).
- ¹⁶ D. Schmidiger, P. Bouillot, S. Mühlbauer, S. Gvasaliya, C. Kollath, T. Giamarchi, and A. Zheludev, Phys. Rev. Lett. **108**, 167201 (2012).
- ¹⁷ A. A. Nersesyan, A. O. Gogolin, and F. H. Eßler, Phys. Rev. Lett. **81**, 910 (1998).
- ¹⁸ T. Vekua and A. Honecker, Phys. Rev. B **73**, 214427 (2006).
- ¹⁹ A. Lavarélo, G. Roux, and N. Laflorencie, Phys. Rev. B **84**, 144407 (2011).
- ²⁰ B. Koteswararao, S. Salunke, A. V. Mahajan, I. Dasgupta, and J. Bobroff, Phys. Rev. B **76**, 052402 (2007).
- ²¹ O. Mentré, E. Janod, P. Rabu, M. Hennion, F. Leclercq-Hugeux, J. Kang, C. Lee, M. H. Whangbo, and S. Petit, Phys. Rev. B **80**, 180413 (2009).
- ²² O. Mentré, E. M. Ketatni, M. Colmont, M. Huvé, F. Abraham, and V. Petricek, J. Am. Chem. Soc. **126**, 10857 (2006).
- ²³ A. A. Tsirlin, I. Rousochatzakis, D. Kasinathan, O. Janson, R. Nath, F. Weickert, C. Geibel, A. M. Läuchli, and H. Rosner, Phys. Rev. B **82**, 144426 (2010).
- ²⁴ B. Koteswararao, A. V. Mahajan, L. K. Alexander, and J. Bobroff, J. Phy. Condens. Matter **22**, 035601 (2010).
- ²⁵ Y. Kohama, S. Wang, A. Uchida, K. Prsa, S. Zvyagin, Y. Skourski, R. D. McDonald, L. Balicas, H. M. Ronnow, C. Rüegg, and M. Jaime, Phys. Rev. Lett. **109**, 167204 (2012).
- ²⁶ B. Keimer, A. Aharony, A. Auerbach, R. J. Birgeneau, A. Cassanho, Y. Endoh, R. W. Erwin, M. A. Kastner, and G. Shirane, Phys. Rev. B **45**, 7430 (1992).
- ²⁷ B. Keimer, N. Belk, R. J. Birgeneau, A. Cassanho, C. Y. Chen, M. Greven, M. A. Kastner, A. Aharony, Y. Endoh, R. W. Erwin, and G. Shirane, Phys. Rev. B **46**, 14034 (1992).
- ²⁸ I. Dzyaloshinsky, J. Phys. Chem. Solids **4**, 241 (1958).
- ²⁹ T. Moriya, Phys. Rev. **120**, 91 (1960).
- ³⁰ I. Affleck and M. Oshikawa, Phys. Rev. B **60**, 1038 (1999).
- ³¹ Y. J. Wang, F. H. L. Essler, M. Fabrizio, and A. A. Nersesyan, Phys. Rev. B , 024412 (2002).
- ³² C. Stock, W. J. L. Buyers, R. Liang, D. Peets, Z. Tun, D. Bonn, W. N. Hardy, and R. J. Birgeneau, Phys. Rev. B , 014502 (2004).
- ³³ M. J. Cooper and R. Nathans, Acta. Cryst. **23**, 357 (1967).
- ³⁴ N. J. Chesser and J. D. Axe, Acta. Cryst. A **29**, 160 (1973).
- ³⁵ The high energy scattering is much broader than the resolution and does not disperse in the \mathbf{Q} -range probed. Since this intensity does not appear in scans performed at equivalent \mathbf{Q} positions in the $(0, k, l)$ plane it is likely spurious scattering resulting from the coarse out-of-plane resolution of the vertically focusing monochrometer.
- ³⁶ P. J. Brown, *International Tables for Crystallography*, Vol. C (Springer, Berlin, 2006) Chap. 4.4.5, pp. 454–461.
- ³⁷ K. Nomura, J. Phys. Soc. Jpn **72**, 476 (2003).
- ³⁸ P. C. Hohenberg and W. F. Brinkman, Phys. Rev. B **10**, 128 (1974).
- ³⁹ M. B. Stone, I. Zaliznyak, D. H. Reich, and C. Broholm, Phys. Rev. B **64**, 144405 (2001).
- ⁴⁰ S. Notbohm, P. Ribeiro, B. Lake, D. A. Tennant, K. P. Schmidt, G. S. Uhrig, C. Hess, R. Klingeler, G. Behr, B. Büchner, M. Reehuis, R. I. Bewley, C. D. Frost, P. Manuel, and R. S. Eccleston, Phys. Rev. Lett. **98**, 027403 (2007).
- ⁴¹ B. Leuenberger, A. Stebler, H. U. Güdel, A. Furrer, R. Feile, and J. K. Kjems, Phys. Rev. B **30**, 6300 (1984).
- ⁴² M. Matsuda, T. Yosihama, K. Kakurai, and G. Shirane, Phys. Rev. B **59**, 1060 (1999).
- ⁴³ G. Xu, C. Broholm, D. H. Reich, and M. A. Adams, Phys. Rev. Lett. **84**, 4465 (2000).
- ⁴⁴ K. Damle and S. Sachdev, Phys. Rev. B **57**, 8307 (1998).
- ⁴⁵ A. Zheludev, V. O. Garlea, L. P. Regnault, H. Manaka, A. Tsvetlik, and J. H. Chung, Phys. Rev. Lett. **100**, 157204 (2008).
- ⁴⁶ B. Náfrádi, T. Keller, H. Manaka, A. Zheludev, and B. Keimer, Phys. Rev. Lett. **106**, 177202 (2011).
- ⁴⁷ A. Zheludev, S. E. Nagler, S. M. Shapiro, L. K. Chou, D. R. Talham, and M. W. Meisel, Phys. Rev. B **53**, 15004 (1996).
- ⁴⁸ M. Kenzelmann, R. A. Cowley, W. J. L. Buyers, and D. F. McMorrow, Phys. Rev. B **63**, 134417 (2001).
- ⁴⁹ G. Xu, C. Broholm, Y.-A. Soh, G. Aeppli, J. F. DiTusa, Y. Chen, M. Kenzelmann, C. D. Frost, T. Ito, K. Oka, and H. Takagi, Science **317**, 1049 (2007).
- ⁵⁰ V. O. Garlea, A. Zheludev, L. P. Regnault, J. H. Chung, Y. Qiu, M. Boehm, K. Habicht, and M. Meissner, Phys. Rev. Lett. **100**, 037206 (2008).
- ⁵¹ S. Miyahara, J. B. Fouet, S. R. Manmana, R. M. Noack, H. Mayaffre, I. Sheikin, C. Berthier, and F. Mila, Phys. Rev. B , 184402 (2007).